ANALYSIS OF GROUND MOTION AMPLIFICATION OF SEDIMENTARY BASINS: STUDY ON THE HEAVILY DAMAGED BELT ZONE DURING 1995 KOBE EARTHQUAKE

Yuzo SHINOZAKI[1] And Kazuhiro YOSHIDA[2]

SUMMARY

A direct three-dimensional(3-D) as well as 2.5-dimensional(2.5-D) boundary element method is applied to evaluate seismic responses in 3-D and 2-D sedimentary basin to estimate the amplification characteristics of the ground motions in the heavily damaged belt zone in Kobe City during the 1995 Hyogo-ken earthquake. We have utilized the Green's functions for an elastic half-space medium to formulate boundary integral equations in terms of displacements and tractions at the medium interface in both 3-D and 2.5-D BEM. We examined in details the effects of different types of incident waves such as plane waves, a single point source, and a moving fault model on the responses of 3-D sedimentary basin and the effects of different types of cross-section of the 2-D sedimentary basin on the spatial variation of ground motions in the 2-D basin taking into account effects of 3-D fault sources.

INTRODUCTION

Kobe city area was attacked by a big earthquake, M7.2, on January 17, 1995. A heavily damaged belt zone extended from Suma-ward, west Kobe, through Nishinomiya city emerged, where the JMA seismic intensity was VII. Some seismic reflection method carried out in the zone after the earthquake revealed that there exists a deep irregular underground structure beneath the damage belt zone. Although there were a very few earthquake recorded within the damaged belt zone, it was inferred that strong ground motion amplifications occurred along the damage belt zone. Since then, many studies on the amplification characteristics of ground motion on a deep irregular underground structure were conducted based on FEM[Motosaka & Nagano, 1996], FDM[Kawase, 1996; Arben et al., 1997], and 3-D BEM[Shinozaki & Yoshida, 1996].

In the present study, at first, we examine seismic waves in a 3-D sedimentary basin for both incident plane waves, and incident waves generated from a single point source and a moving fault. A direct boundary element method is applied to evaluate seismic waves in a 3-D sedimentary basin. We have utilized the Green's functions for an elastic half-space medium calculated by one of the authors, who verified the accuracy of the Green's functions through comparison of the numerical results with those obtained by other method. Since the boundary conditions at the free surface of elastic media are automatically satisfied, the direct 3-D boundary element method is precisely formulated through those Green's functions based on the boundary conditions along an arbitrarily shaped medium interface. Secondly, we applied a direct 2.5 dimensional element method to evaluate ground motions in 2-D sedimentary basin due to a three-dimensional moving fault to estimate quantitatively the effects of different types of cross-section of the 2-D sedimentary basin on the strong ground motions in the 2-D basin.

2. METHOD OF ANALYSIS

2.1 3-D model

[1]   Department of Architecture, Kyoto University, Kyoto, JAPAN, Email: sinozaki@archi.kyoto-u.ac.jp
[2]   Izumi Research Institute, Shimizu Corp., Chiyoda, Tokyo, JAPAN

Geometry of the 3-D model is shown in Figure 1. A sedimentary basin is assumed to be a 3-D model (denoted by medium 1) , which is characterized by mass density, ρ_1, compressional wave velocity, α_1, and shear wave velocity, β_1. Medium 1 is surrounded by a half-space medium (denoted by medium 2), which is characterized by mass density, ρ_2 , compressional wave velocity, α_2, and shear wave velocity, β_2. An interface between the media 1 and 2 is denoted by S and perfect bonding along the interface is understood. The material of them is assumed to be linearly elastic, homogeneous and isotropic. Starting with Betti's reciprocity theorem, we obtain the following BEM equations in terms of unknown displacement $u_j(\mathbf{x})$ and traction $p_j(\mathbf{x}, \mathbf{n})$ of the boundary S as follows:

$$\frac{1}{2} \cdot u_i^{(2)}(\mathbf{x}^*) - \int\int_S \left\{ G_{ji}^{(2)}(\mathbf{x}; \mathbf{x}^*) \cdot p_j^{(2)}(\mathbf{x}, \mathbf{n}) - H_{ji}^{(2)}(\mathbf{x}, \mathbf{n}; \mathbf{x}^*) \cdot u_j^{(2)}(\mathbf{x}) \right\} dS = u_i^{inc}(\mathbf{x}^*) \tag{1}$$

$$\frac{1}{2} \cdot u_i^{(1)}(\mathbf{x}^*) + \int\int_S \left\{ G_{ji}^{(1)}(\mathbf{x}; \mathbf{x}^*) \cdot p_j^{(1)}(\mathbf{x}, \mathbf{n}) - H_{ji}^{(1)}(\mathbf{x}, \mathbf{n}; \mathbf{x}^*) \cdot u_j^{(1)}(\mathbf{x}) \right\} dS = 0 \tag{2}$$

in which $G_{ji}(\mathbf{x}; \mathbf{x}^*)$ and $H_{ji}(\mathbf{x}, \mathbf{n}; \mathbf{x}^*)$ are the $j-$th components of displacement and traction at $\mathbf{x}$ due to a point force in the $i-$th direction at $\mathbf{x}^*$, and $\mathbf{n}$ is a unit outward normal of the boundary S , where, the superscript (m) $(m = 1, 2)$ denotes the medium number. The inhomogeneous term $u_i^{inc}(\mathbf{x}^*)$ is an incident wavefield. If we assume a double couple source model of earthquake, it is expressed by the following equation by using the moment tensors and the first derivatives of the Green's function:

$$u_i^{inc}(\mathbf{x}^*) = M_{jk} \cdot G_{ij,k} \tag{3}$$

where $G_{ij,k}$ is the first derivative of G_{ij} with respect to the k-component. For a more general finite fault model, the displacement can be expressed by the superposition of Equation (3).
Equations (1) and (2) are combined using the boundary conditions prescribed by,

$$u_j^{(1)}(\mathbf{x}) = u_j^{(2)}(\mathbf{x})$$
$$p_j^{(1)}(\mathbf{x}, \mathbf{n}) = p_j^{(2)}(\mathbf{x}, \mathbf{n}) \tag{4}$$

To solve Equations (1) and (2), the discretization scheme of both boundary shape and boundary values $u_j(\mathbf{x})$ and $p_j(\mathbf{x}, \mathbf{n})$ should be introduced in the same manner as the finite element method.
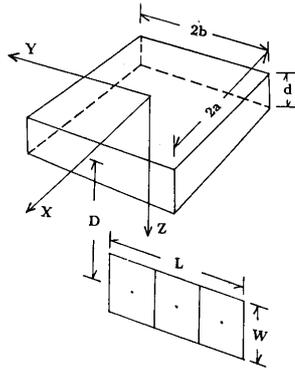
Figure 1: 3-D sedimentary basin model.　　　　Figure 2: 2.5-D sedimentary basin model.
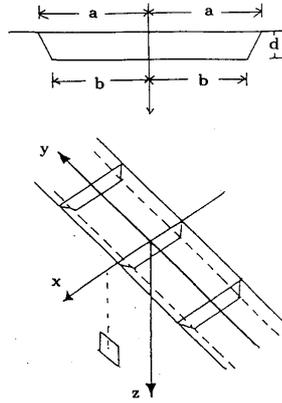
2.2 2.5-D model

Geometry of the 2.5-D model is shown in Figure 2. It is the same model as the 3-D model except a sedimentary basin being assumed to be a 2-D model. Following a similar procedure as 3-D model, we obtain the following BEM equations in terms of unknown displacement $\tilde{u}_j(\mathbf{x})$ and traction $\tilde{p}_j(\mathbf{x}, \mathbf{n})$ of the boundary Γ corresponding to Equations (1) and (2) as follows[Fujiwara, 1996]:

$$\frac{1}{2} \cdot \tilde{u}_i^{(2)}(\mathbf{x}^*) - \int_\Gamma \left\{ \tilde{G}_{ji}^{(2)}(\mathbf{x}; \mathbf{x}^*) \cdot \tilde{p}_j^{(2)}(\mathbf{x}, \mathbf{n}) - \tilde{H}_{ji}^{(2)}(\mathbf{x}, \mathbf{n}; \mathbf{x}^*) \cdot \tilde{u}_j^{(2)}(\mathbf{x}) \right\} d\Gamma = \tilde{u}_i^{inc}(\mathbf{x}^*) \tag{5}$$

$$\frac{1}{2} \cdot \tilde{u}_i^{(1)}(\mathbf{x}^*) + \int_\Gamma \left\{ \tilde{G}_{ji}^{(1)}(\mathbf{x}; \mathbf{x}^*) \cdot \tilde{p}_j^{(1)}(\mathbf{x}, \mathbf{n}) - \tilde{H}_{ji}^{(1)}(\mathbf{x}, \mathbf{n}; \mathbf{x}^*) \cdot \tilde{u}_j^{(1)}(\mathbf{x}) \right\} d\Gamma = 0 \tag{6}$$

The tilde in the equations denotes the Fourie transforms of $u_i(\mathbf{x})$, $p_i(\mathbf{x})$, $G_{ji}(\mathbf{x};\mathbf{x}^*)$, $H_{ji}(\mathbf{x},\mathbf{n};\mathbf{x}^*)$, and they are defined by

$$\tilde{u}_j(\omega; x, k_y, z) = \int_{-\infty}^{\infty} u_j(\omega; x, y, z) e^{ik_y y} dy \tag{7}$$

$$\tilde{p}_j(\omega; x, k_y, z', \mathbf{n}) = \int_{-\infty}^{\infty} p_j(\omega; x, y, z', \mathbf{n}) e^{ik_y y} dy \tag{8}$$

$$\tilde{G}_{ji}(\omega; x', k_y, z'; x, 0, z) = \int_{-\infty}^{\infty} G_{ji}(\omega; x', y', z'; x, 0, z) e^{ik_y y'} dy' \tag{9}$$

$$\tilde{H}_{ji}(\omega; x', k_y, z', \mathbf{n}; x, 0, z) = \int_{-\infty}^{\infty} H_{ji}(\omega; x', y', z', \mathbf{n}; x, 0, z) e^{ik_y y'} dy' \tag{10}$$

To solve Equations (5) and (6), the discrete wave number method is used[Bouchon & Aki, 1977].

3. NUMERICAL RESULTS

3.1 3-D model

We considered the incidence of plane waves of the P, SH, and SV waves. It is assumed that the length, width, and depth of a rectangular sedimentary basin are $2a = 2b = 10$km and $d = 1$km, respectively, and shear wave velocities of media 1 and 2 are $\beta_1 = 1.575$km/sec and $\beta_2 = 3.5$km/sec with Poisson's ratios $\nu_1 = 0.3$ and $\nu_2 = 0.242$, respectively. From frequency domain results, we computed synthetic seimograms using the FFT algorithm. Figure 3 show synthetic seismograms for surface displacements at 79 sites equally spaced along the x axis of the 3-D sedimentary basin due to plane SH or SV Ricker wavelets with a characteristic period of 2.0 sec. The magnitude of peak response at each time history is indicated as the length of time axis marked with a symbol   , whose maximum value is adjusted to the duration of 40 seconds. We have $u_x = u_z = 0$ along the x axis of the sedimentary basin because of the symmetry of the problem for the case of SH wave incidence. Those responses clearly show propagation of Love waves generated from edge of the sedimentary basin. It should be noted seismic responses of 3-D sedimentary basin for the case of incident plane waves do not show such a significant amplification near the edge of the basin as shown in Figure 6 for the case of a moving fault source.

Figure 4 show synthetic seismograms for surface displacements u_z and u_x at 79 sites along the x axis of the sedimentary basin due to a point source located at (x=6km, y=0, z=5km) excited in the x direction. Surface displacement u_y vanish along the x axis for the case of this excitation. Source time function is a Ricker wavelet with a characteristic period of 2.0 sec. Material properties for media 1 and 2 are assumed to be the same values as the ones shown in Figure 3. In the left side of the figure, the cross-section of the basin along the x direction is shown. It is seen that body waves, $i.e.$, SV waves, first arrive at the sites and then Rayleigh waves generated from the basin edge propagate forward along the longitudinal direction, however, no little Rayleigh waves reflected from the other basin edge propagate backward.

We assume a moving fault model (i.e., dip angle $\delta = 90°$, rake angle $\lambda = 180°$, strike angle $\phi = 90°$) enclosed by ($x = 6$km, -13.5km $\leq y \leq -7.5$km, 9km $\leq z \leq 11$km). Figure 5 shows velocity responses of three components u_z, u_x and u_y along the x axis of an elastic half-space without a sedimentary basin for the Rise time=2.0sec. The fault-normal component u_x is most amplified due to the directivity effect of moving fault model. Three surface velocity components u_z, u_x, and u_y along the x axis of the 3-D sedimentary basin due to a moving fault are shown in Figure 6. Every component of surface responses near the basin edge is deamplified due to the constraint effect of the hard half-space. The fault-normal component u_x , which is amplified at least twice as much as other components u_y and u_z , is most amplified about 2.0km distant from the basin edge, and after that site decay gradually. Since these spatial variations of surface ground motions of 3-D sedimentary basin due to a moving fault are similar to those of 2.5-D sedimentary basin as shown in Figure 7, both basin edges in the 3-D model normal to the fault plane do not seem to have significant effects on the surface ground motions.

3.2 2.5-D model

Though a sedimentary basin model as shown in Figure 2 is assumed to be a two-dimensional problem, however, incident wavefields should be considered as a three-dimensional problem, therefore, we have to take into account three-dimensional spatial variations of ground motions along y axis on 2-D sedimentary basin.
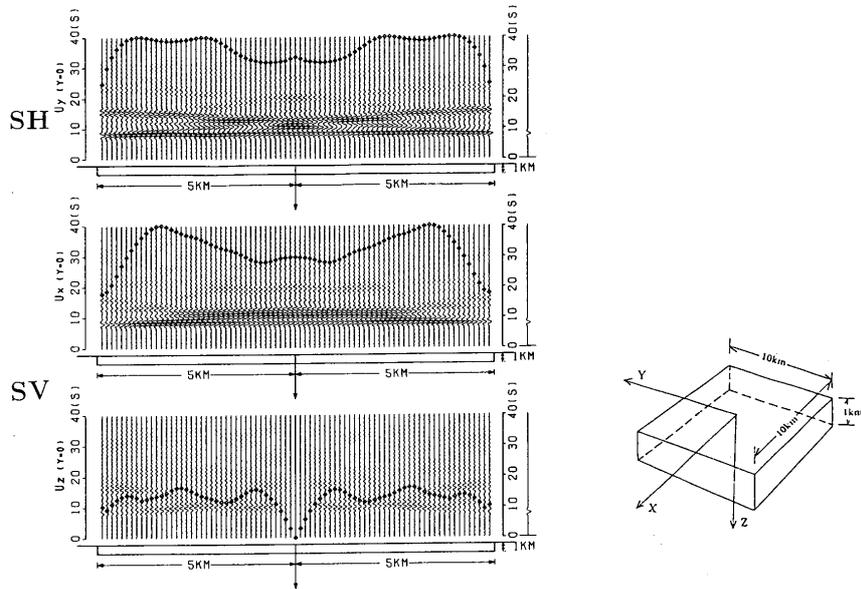
Figure 3: Time-domain responses for surface displacements at 79 sites equally spaced along the x axis of the 3-D sedimentary basin due to vertically propagating plane SH or SV waves. Source time function is a Ricker wavelet with a characteristic period of 2.0 sec.
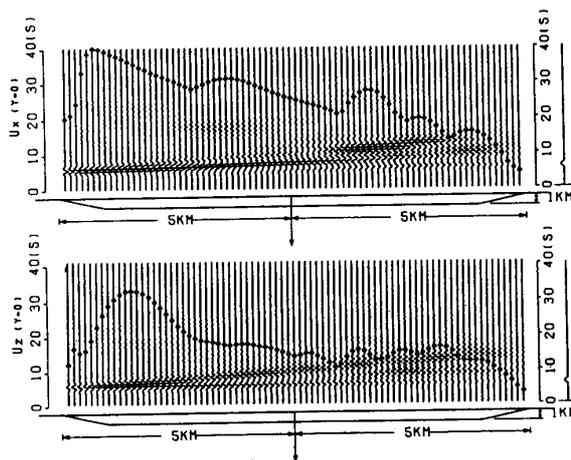
Figure 4: Time-domain responses for surface displacements u_z and u_x at 79 sites equally spaced along the x axis of the 3-D sedimentary basin due to a single point source excited in the x direction located at (x=6km, y=0, z=5km). Source time function is a Ricker wavelet with a characteristic period of 2.0 sec.

4
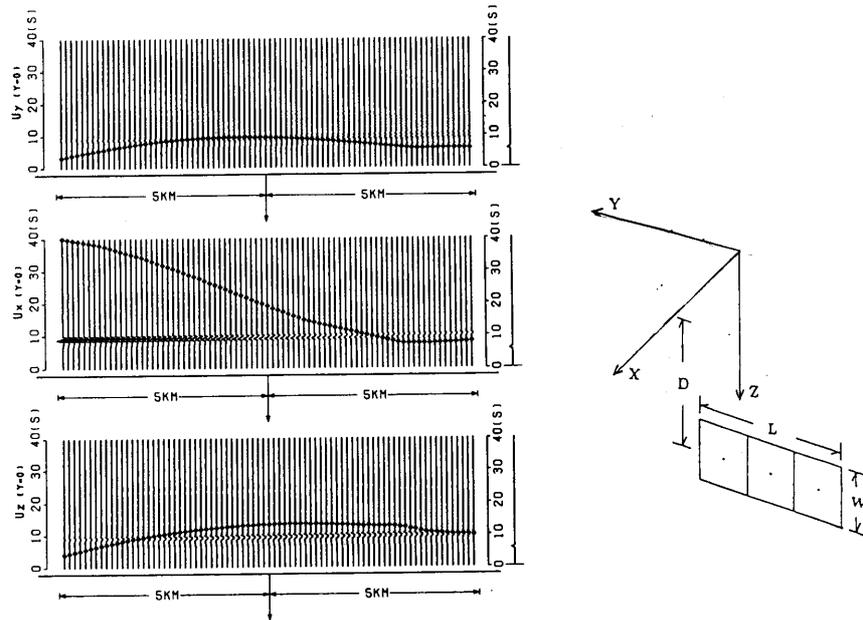
Figure 5: Time-domain responses for surface velocities u_z, u_x, and u_y at 79 sites equally spaced along the x axis of the Half-Space due to a moving fault (i.e., dip angle $\delta = 90°$, rake angle $\lambda = 180°$, strike angle $\phi = 90°$) at (x = 6km, -13.5km $\leq$ y $\leq$ -7.5km, 9km $\leq$ z $\leq$ 11 km). Rise time is 2.0sec and rupture velocity is 2.8km/sec.
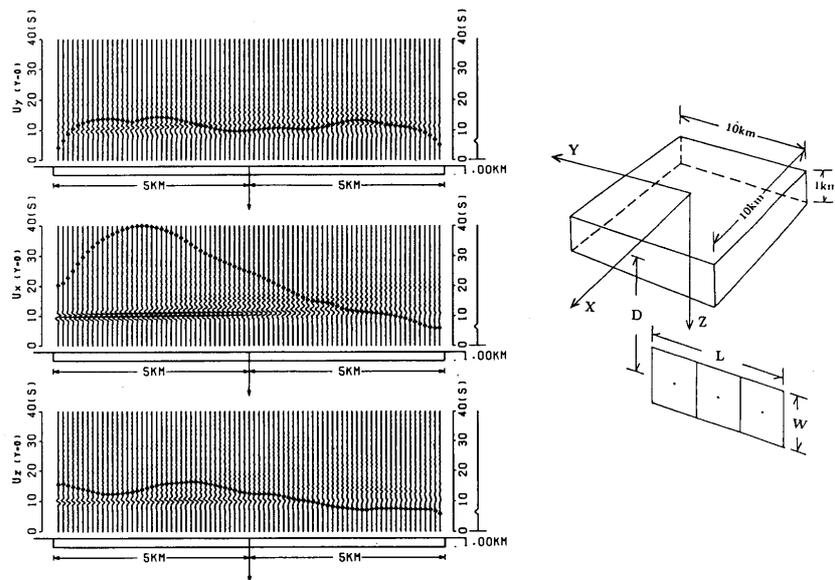
Figure 6: Time-domain responses for surface velocities u_z, u_x, and u_y at 79 sites equally spaced along the x axis of the 3-D sedimentary basin due to a moving fault (i.e., dip angle $\delta = 90°$, rake angle $\lambda = 180°$, strike angle $\phi = 90°$) at (x = 6km, -13.5km $\leq$ y $\leq$ -7.5km, 9km $\leq$ z $\leq$ 11 km). Rise time is 2.0sec and rupture velocity is 2.8km/sec.

5
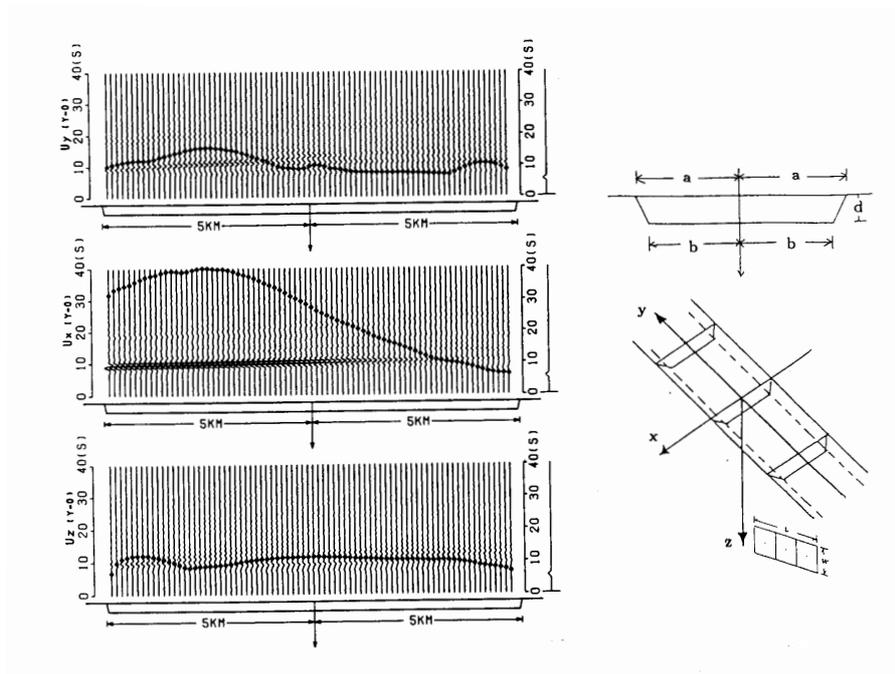
Figure 7: Time-domain responses for surface velocities u_z , u_x , and u_y at 79 sites equally spaced along the x axis of Model B basin due to a moving fault (i.e., dip angle $\delta = 90°$, rake angle $\lambda = 180°$, strike angle $\phi = 90°$) at (x = 6km, -13.5km $\leq$ y $\leq$ -7.5km, 9km $\leq$ z $\leq$ 11 km). Rise time is 2.0sec and rupture velocity is 2.8km/sec.
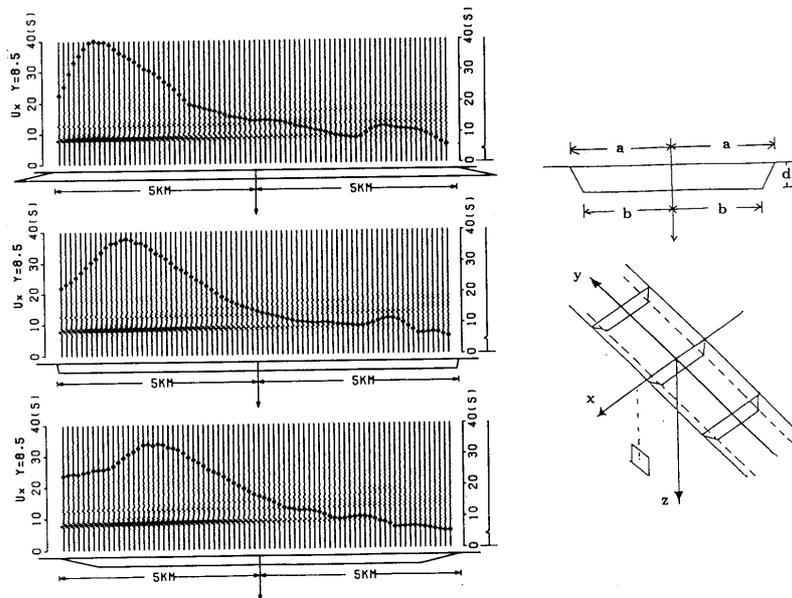
Figure 8: Effect of shape of 2-D basin edge on time-domain responses for fault-normal component surface velocity u_x along the y=8.5km due to a double couple force(i.e., dip angle $\delta = 90°$, rake angle $\lambda = 180°$, strike angle $\phi = 90°$)) at (x=6km, y=0km, z=10km). Rise time is 1.0sec.

Model A   Model B   Model C
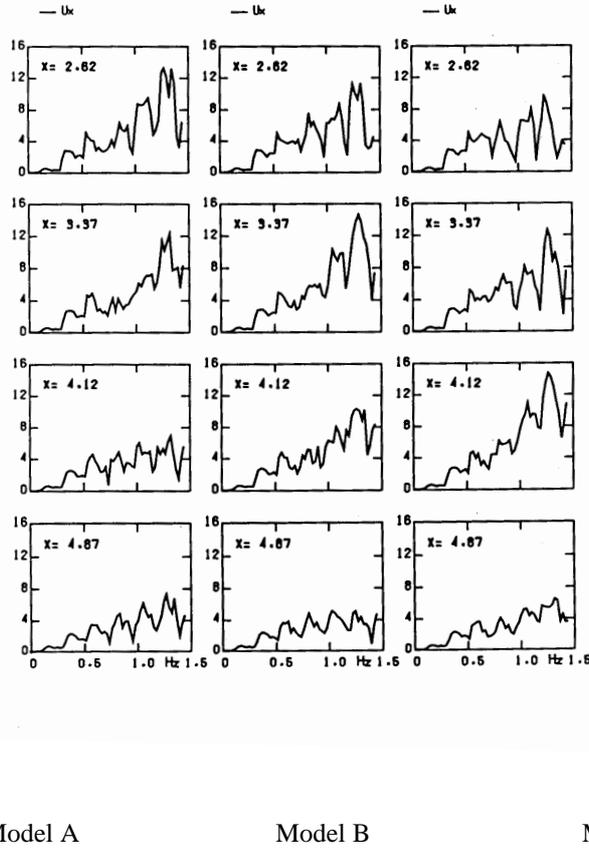
Figure 9: Amplitude characteristics of transfer functions for fault-normal component surface velocity u_x along the y=8.5km of 2-D basin model due to a double couple force. The fault parameters are the same as shown in Figure 8.

Three different types of cross-section of 2-D sedimentary basin model are assumed as follows(model parameters a; basin surface width, b; basin bottom width):
1)Model A: a=5km, b=4km, d=1km
2)Model B: a=5km, b=5km, d=1km
3)Model C: a=5km, b=6km, d=1km
The P and S wave velocities of the soil media are the same as those of 3-D model.

Figure 7 shows three surface velocity components u_z, u_x, and u_y along the x axis of Model B basin due to a moving fault(i.e., dip angle $\delta = 90°$, rake angle $\lambda = 180°$, strike angle $\phi = 90°$) enclosed by ($x = 6$km, -13.5km $\leq y \leq$ -7.5km, 9km $\leq z \leq$ 11km). These results were calculated based on the same fault source model shown in Figure 6. The difference between them lies in the basin model, i.e., 3-D model or 2-D model. According as the rise time decreases, the spatial variation of the fault-normal component of peak ground velocity marked with a symbol   , become sharp, and the most amplified site shifts nearer to the basin edge. Even though a sedimentary basin model as well as a fault source model is simplified one, those strong amplifications of fault-normal ground motion near the basin edge seem to elucidate qualitatively the cause of the heavily damaged belt zone. Figure 8 shows synthetic seismograms of fault-normal component velocity u_x along y=8.5km 2.5-D sedimentary basin due to a 3-D double couple force located at (x=6km, y=0km, z=10km). It shows effects of different type of cross-section of 2-D sedimentary basin model. It should be noted that Model C amplified about 20% than Model A shows the most sharp amplification at about 1km distant nearer to the edge of the basin than Model A.

It is important to examine time domain responses as well as frequency domain responses of ground motion to consider effects of different shape of basin edge on the spatial variation of ground motion shown in Figure 8. Figure 9 shows the amplitude characteristics of transfer functions in Model A, B, and C corresponding to the results shown in Figure 8. Those ampitude characteristics of each model show a similar response in the lower

7

frequency range, because ground motion is not influenced with the shape of basin edge in the longer wavelength range compared with the size of basin edge. However, according as the frequency increses, the peak response is shifted from x=2.62km in Model A to x=4.12km in Model C.

4. CONCLUSIONS

A direct three-dimensional(3-D) as well as 2.5-dimensional(2.5-D) boundary element method is applied to evaluate seismic responses in 3-D and 2-D sedimentary basin to estimate the amplification characteristics of the ground motions in the heavily damaged belt zone in Kobe City during the 1995 Kobe earthquake. From the numerical results, it is concluded as follows:

1. Some time domain responses of 3-D sedimentary basin due to incident plane SH waves show that body waves, i.e., SH waves, first arrive at the sites and then Love waves generated from the basin edge propagate forward along the longitudinal direction and propagate backward reflected from the other basin edge.

2. The numerical results for the case of incident plane waves do not show such a significant amplification near the edge of the basin as shown in the heavily damaged belt zone during the 1995 Kobe earthquake.

3. The normal component of the fault due to a moving fault is amplified at least twice as much as other components due to the directivity effect of moving fault model. These spatial variations of ground motion amplification appear to be the same tendency as those of the uniform elastic half-space without the basin except some zone near the basin edge.

4. Even though a sedimentary basin model as well as a fault source model is simplified one, these strong amplifications of fault-normal ground motion near the basin edge seem to elucidate qualitatively the cause of the heavily damaged belt zone.

5. Three different models of 2-D sedimentary basin are assumed to estimate the basin edge effects on ground motions of sedimentary basin. It should be noted that Model C which is amplified about 20% than Model A shows the most sharp amplification at about 1km distant nearer to the edge of the basin than Model A.

5. ACKNOWLEDGMENTS

6. REFERENCES

Bouchon, M. and K. Aki(1977),"Discrete wave-number representation of seismic-source wave fields", *Bulletin of Seismological Society of America,* 67, pp.259-277.

Fujiwara, H.(1996),"Three-dimensional wavefield in a two-dimensional basin structure due to point source", *Journal of Physics of the Earth*, 44, pp.1-22.

Kawase, H.(1996),"The cause of the damage belt in Kobe: '' The basin-edge effect,'' constructive interference of the direct S-wave with the basin-induced diffracted/Rayleigh waves", *Seismological Research Letters*, 67, pp.25-34.

Motosaka, M. & M. Nagano(1997),"Analysis of amplification characteristics of ground motions in the heavily damaged belt zone during the 1995 Hyogo-ken nanbu earthquake", *Earthquake Engineering Structural Dynamics*, 26, pp.377-393.

Pitarka, A., et al.(1996),"Basin structure effects in the Kobe area inferred from the modeling of ground motions from two aftershocks of the January 17, 1995, Hyogoken-nanbu earthquake", *Journal of Physics of the Earth*, 44, pp.563-576.

Shinozaki, Y. & K. Yoshida(1996),"Seismic waves in 3-D sedimentary basins due to point source",*Proceedings of 11th World Conference on Earthquake Engineering, Paper No.1175.*